The Electric Field of the Sun and Solar Wind

C. Fred Driscoll,
UCSD Physics

AGU/fm2020 / SH029.20

Electric fields are endemic to plasmas, and are often concentrated in Sheaths, resulting in particle acceleration.

Here, electric effects are calculated for the Solar interior, photosphere, and corona, based on standard 1-D radial models by Bahcall (2005) and Fontenla (1993) . The major uncertainty is in the photon-electron scattering cross-section $\sigma_{\gamma e}$ for re-combining (i.e. correlated) plasmas.

A reasonable estimate for $\sigma_{\gamma e}$ shows that electric fields in the photospheric sheath and corona can accelerate protons out of the 2keV gravity well and up to the 1.3 keV energies observed in the Solar Wind. The light scattering from the accelerating proton/electron wind approximates that attributed to a hot, hydrostatic K-Corona. Energetically, this requires about 10^{-6} of the thermal photon flux of the sun.

The 1-D radial model identifies the energetics as thermo-electric and photo-electric; but a more realistic model would include surface granulation on the 0.5Mm scale, and would probably show filamentary beams with diameters down to the 10.km scale. The inevitable small charge imbalances would generate strong magnetic fields, and filament clumping would increase the visibility and impact of the small beams.

Supported by UCSD and AFOSR
NNP.ucsd.edu/Solar/

Equlibrium Stellar Fluid Eqns:

mass	charge	photons
$m_p\ m_e$	$e^-\ p^+$	γ

1 $\nabla^2\Psi(r) = G\, m_p\, n_p(r)$ Gravity

2 $\nabla\bullet\Gamma_\varepsilon(r) = \frac{d}{dt}\varepsilon(r)$ Fusion Energy Flux

3 $-(4aT^3)\,T'(r)\; l_\gamma = \frac{4}{c}\Gamma_\varepsilon$ Thermal Energy Diffusion

4a $[n_pT]' \qquad + n_p m_p \Psi' + (+e)n_p\Phi' = 0$ Proton Fluid Momentum

Thermo- Photo- Electric

4b $[n_eT]' - \frac{\Gamma_{\varepsilon\gamma}}{c\, l_{\gamma e}} + \cancel{n_e m_e\Psi'} + (-e)n_e\Phi' = 0$ Electron Fluid Momentum

---

4a+4b $[(2n)T]' - \frac{\Gamma_{\varepsilon\gamma}}{c\, l_{\gamma e}} + n\, m_p\Psi' = 0$ Total Fluid Momentum

4a−4b $\frac{\Gamma_{\varepsilon\gamma}}{c\, l_{\gamma e} n_e} + m_p\Psi' + (2e)\Phi' = 0$ Electric Field

---

$$-m_p g(r)/2 \approx eE_{\mathrm{Th}}(r)$$

Thermo-Electric in high-density collisional regime

A. Pannekoek
S. Rosseland (1924)
A.E. Eddington

$$\sigma_{\gamma e} \equiv \frac{1}{l_{\gamma e} n_e}$$

$$\frac{\Gamma_{\varepsilon\gamma}}{2c}\sigma_{\gamma e} = eE_\gamma$$

Photo-Electric : Photons de-coupled from T' and ψ'
γ/e- cross-section is large for *correlated* e-/p+

Electric effects in 2 standard models, Core & Photosphere

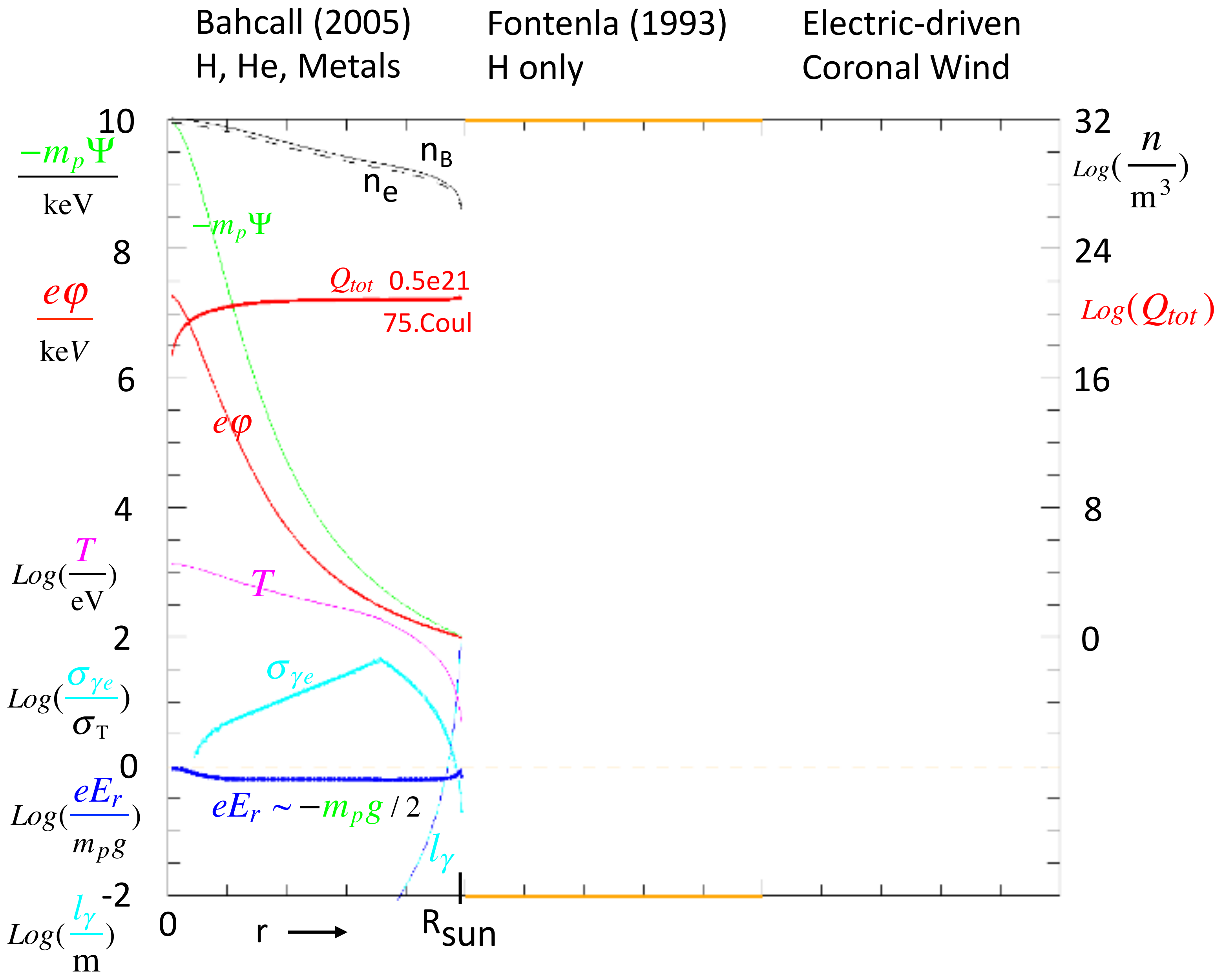

Bahcall 2005

Baryon and electron densities (n_B, n_e) decrease from 10^32 at r=0 to 10^26 at Rsun-12.Mm , creating a 10.keV gravity well Ψ. Temperature T decreases from 1.4keV to 7.eV, and photon absorption length $l\gamma$ increases from sub-meter (not shown) to 100.m .

The gradient in electron pressure n_eT implies a thermo-electric force eE_r ~ $m_pg/2$ on each proton., and an electric potential drop of $\Delta e\phi$~5.keV.

The absorption length $l\gamma$ implies a photon-election cross-section $\sigma_{\gamma e}$ varying between the Thomson σ_T and 30 σ_T .

The accumulated (positive) charge excess is then Q~0.5e21, or 75.Coulombs

Electric effects in 2 standard models, Core & Photosphere

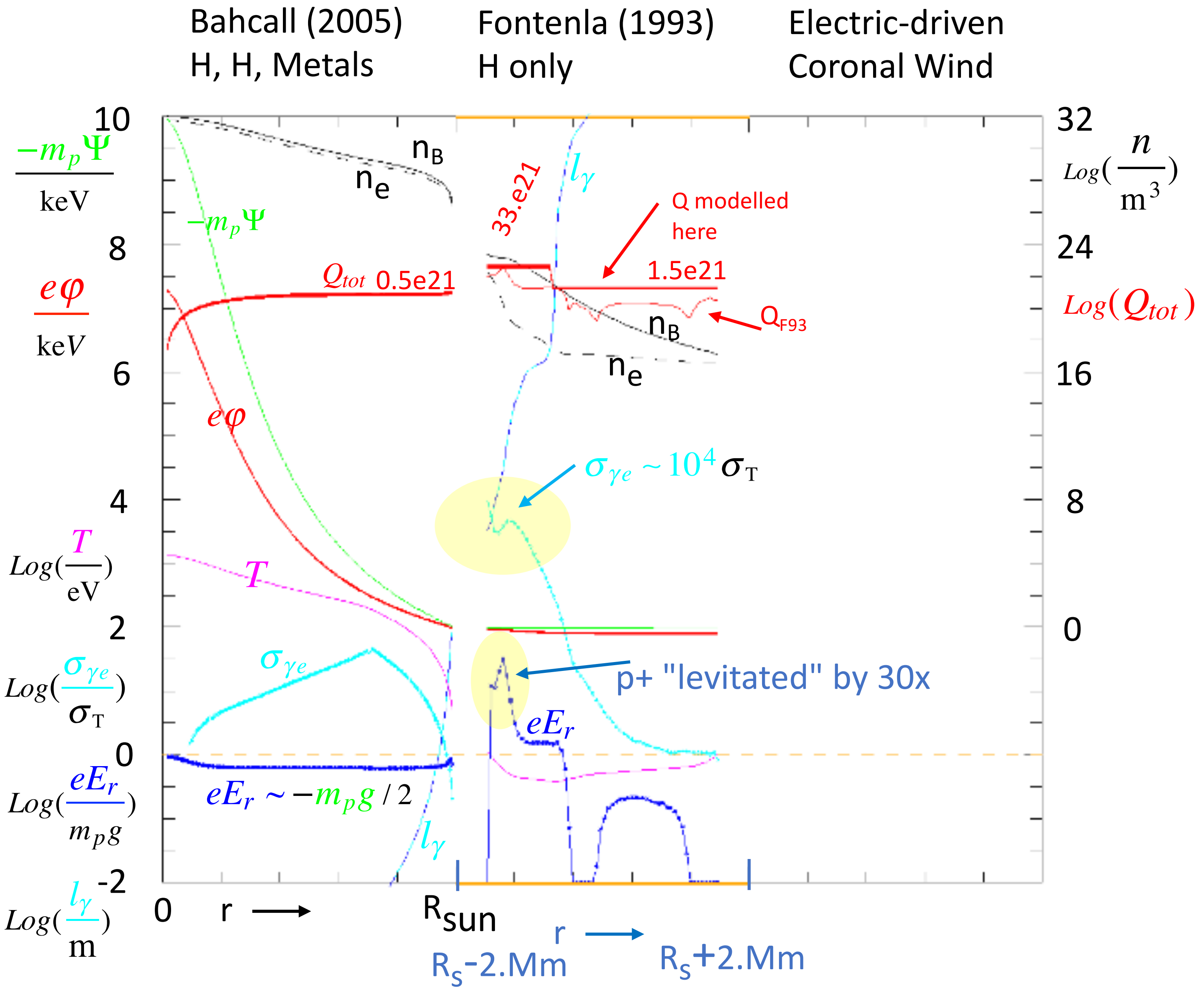

Fontenla 93

This Hydrogen-only model of the photosphere begins at Rs-1.Mm, where n_B~1.3e23, and T~0.8eV .
Over the next 2.Mm, the density drops by 6 decades to n_B~1.5e17, and the "temperature" drops to T~0.4eV before rising precipitously for r > Rs+2.Mm (not shown).

In the photosphere, the photon absorption length l_γ varies from 1e4 to 1e10 meters, as the plasma varies from fully ionized to 1e-4 ionized, and back to largely ionized.

In this critical region of strong e-/p+ correlation, the (derived) photon-electron cross section is as large as 1e4 σ_T, although this was not considered in the model.

More strikingly, the radial electric force eE_r becomes so large as to "levitate" every proton by 30x gravity, i.e. E_r~30 *2.8eV/Mm. Here, the bare proton density is 1e-4 of the neutral H density, so only "runaway" protons can gain energy E_0~ 100.eV .

The derived charge density Q_{F93} has little significance, and the simpler "step charge" model is treated here.
A step of Q~33.e21 over 1.Mm in radius requires charge densities Δn~5.e-3/m^3, which is "small" by any measure.

Electric effects in 2 standard models, Core & Photosphere & Corona Model

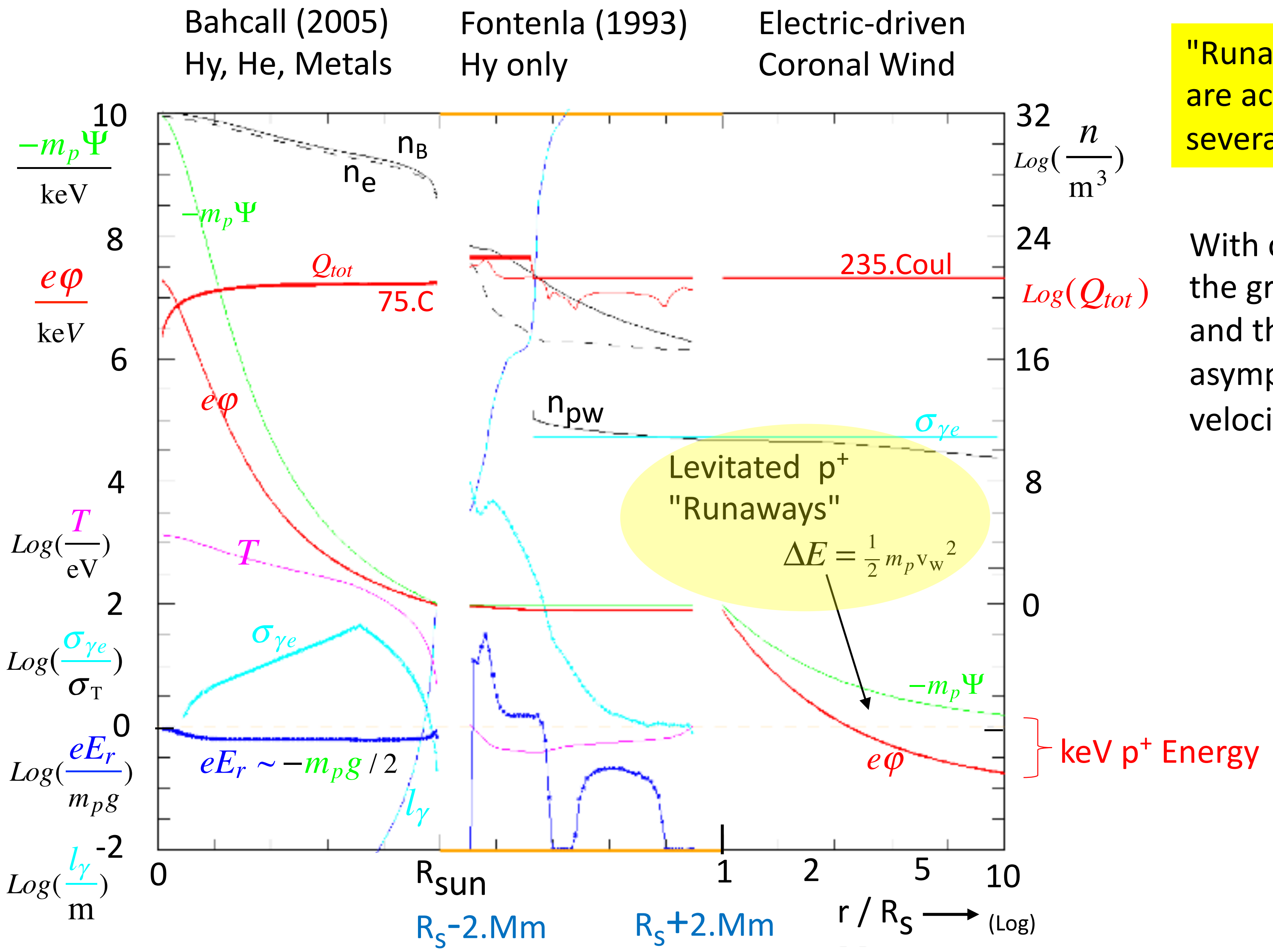

"Runaway" protons with weak H drag are accelerated up to keV energies over several solar radii .

With constant Qtot, the electric field and the gravitational field both fall of as r-2 , and the Solar Wind kinetic energy asymptotes to KE~1.3keV with velocity v_{pw}~500.km/s.

Force Balance with Electric Fields

Ohm's ~~Law~~
Ohm's Balance

E $\quad \langle \tilde{E}_{\text{collision}} \rangle_t = \rho J$ (aka "friction")

$$\rho = \frac{m_e}{e^2} \frac{\nu_{\text{collision}}}{n_e}$$

Ohm's "Law" expresses the *balance* between the external accelerating field E and "frictional drag" which is actually the average of the fluctuating electric collision forces $\langle E_{\text{collision}} \rangle_t$, these being proportional to the current J .

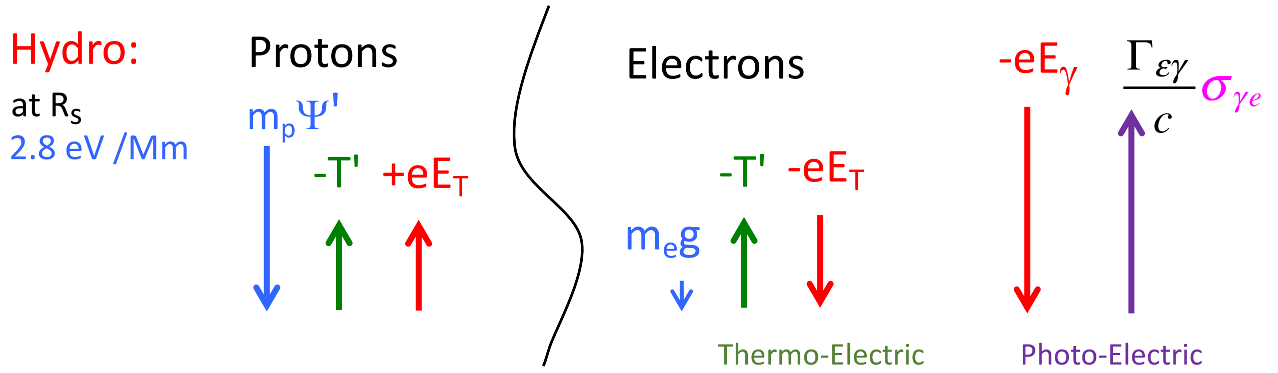

The Thermo-Electric force eE_T arises to balance the (outward) electron pressure gradient T' per electron. It balances the pressure even in the absence of electron current. It can be envisioned as a "drag" on the electrons from the outward thermal flux.

The Photo-Electric force eE_γ arises to balance the (outward) drag on the electrons from the outward photon flux. It arises even in the absence of a particle current or electric current; but in low-collisionality sheaths, the protons are generally accelerated.

Photon-electron scattering cross-section $\sigma_{\gamma e}$ increases with plasma density & correlation.

e- p+ Strongly Corelated "atomic"

Rydberg Hy $\sigma_a(\gamma, H^*) \sim \pi a_0^2 = 0.6 \times 10^{-20}\,\mathrm{m}^2$

Hy neg Ion $\sigma_a(\gamma, H^-; \quad bf) \sim 0.5 \times 10^{-20}\,\mathrm{m}^2$

Hy free-free $\sigma_a(\gamma, H + e^-; ff) \sim 0.5 \times 10^{-20}\,\mathrm{m}^2$

e-/p+/Γγ Bremsstrahlung collisions

$$\sigma_\beta \sim \sigma_M \frac{n_p}{3 \times 10^{23}} E_e^{-1/2}$$

$$\sigma_M \equiv 3.4 \times 10^{-24} = \text{Model}$$

isolated electron

Thomson cross-section

$$\sigma_T = 0.7 \times 10^{-28}\,\mathrm{m}^2$$

The photon-electron absorption/scattering cross-section $\sigma_{\gamma e}$ varies by about 8 decades, depending on the elecron correlation with more massive charges.

Atomic cross-sections, including Hy Rydberg and Hy Negative Ion, dominate throughout the photosphere.

Bremsstrahlung photon scattering occurs during particle collisions, increasing with the density of ions, and increasing as the electron energy E_e decreases (towards recombination).

The modelled σ_M represents an *average* over density clumping, current filamentation, and recombination/heating processes, which are outside the simple 1-D radial model.

"1-d PIC Sim" : Collisional e-p+ Source, Photon Force, H^0 Drag, e- p+ Kinetics, Poisson Eqn => e- p+ Beam

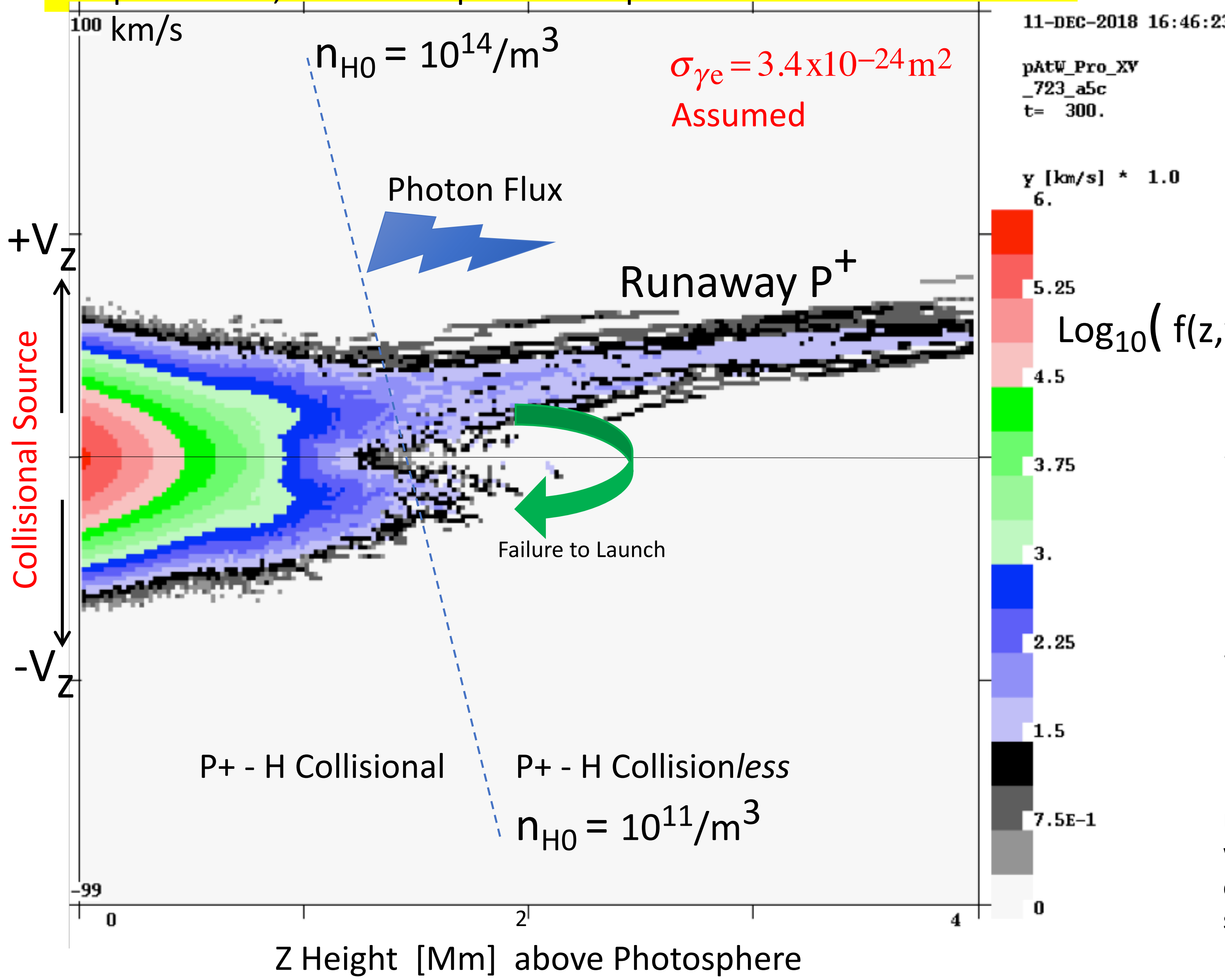

Photo-Electric:

When Electric Field on Protons Exceeds Collisional Drag from H^0 → Runaway p+ :

"Runaway" proton beams are endemic to "confined" plasmas, where the electrons tend to escape faster than the protons.

The plasma-edge "Bohm" sheaths concentrate electric fields, generally so as to retard electrons and accelerate protons. This is especially evident when gravity attracts the protons 1836 times more than the electrons.

The sheath electric fields depend critically on space charge, and steady-state solutions require equality of proton and electron currents.

In realistic 3-D plasmas with surface granulation and neutral current filamentation into "rays", exceedingly weak +/- current imbalance will create significant space charge potentials, driving surface currents and creating surface magnetic fields.

Photon-Driven Solar Wind p+ Flux, Density, Velocity, Energy assuming average $\sigma_{\gamma e} = 3.4 \times 10^{-24}\,\mathrm{m}^2$

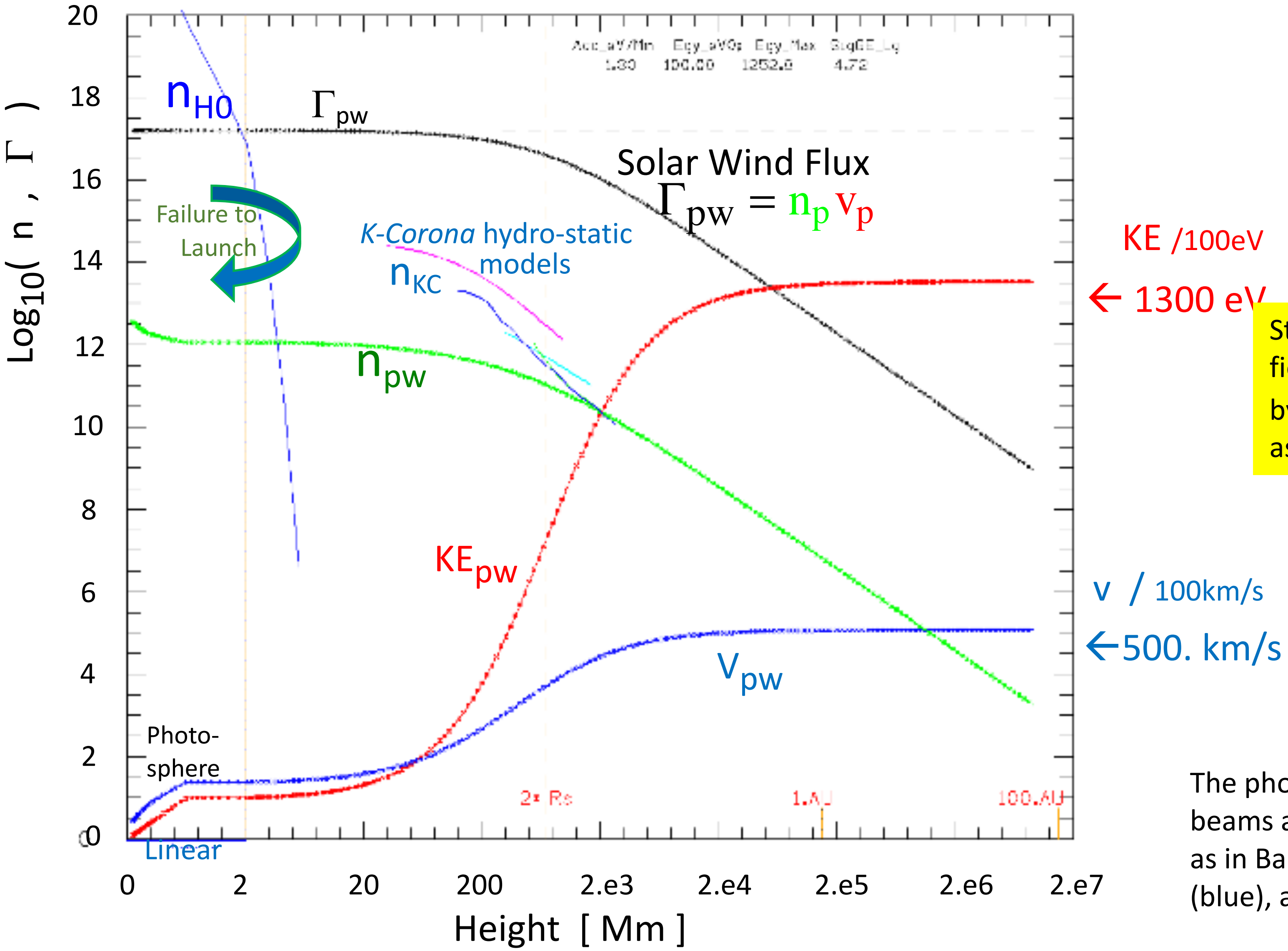

$$\frac{d}{dr}\varepsilon_p = -m_p\Psi' + eE(r) - \cancel{\nu}_c(p^+, H^0)$$

$$\varepsilon_{p+}(\rho) \sim \varepsilon_0 + (1.3\mathrm{keV})\left[1 - 1/\rho\right]$$

$$v_p(\rho) \sim (500.\mathrm{km/s})\left[1 - 1/\rho\right]$$

$$n_p(\rho) \sim 3 \times 10^{11}\ \rho^{-2}\ \mathrm{m}^{-3}$$

$$\Gamma_p(\rho) \sim 1.6 \times 10^{17}\ \rho^{-2}\ \mathrm{s}^{-1}\mathrm{m}^{-2}$$

$$\rho \equiv r / R_s$$

Starting in the photosphere, thermo- and photo-electric fields accelerate a "runaway" beam of protons, neutralized by electrons. With the modelled $\sigma_{\gamma e}$, the proton energy asymptotes to 1.3keV within several solar radii.

A more detailed 3-dim model would include beam "pinching" and filamentation, well below the Mm scale of solar surface granulations.

The photon coupling $\sigma_{\gamma e}$ depends strongly on e-/p+ correlation and density, so some beams would return to the solar surface ("failure to launch").

The photon scattering from from the launched and returning beams appears as the K-Corona, without hydro-static heating, as in Badalyn 1985 (magenta), Strachan 1993 (cyan), Fisher 1995 (blue), and Cranmer 1999 (green).

Solar Wind Magnetic Fluctuations Diagnosing Local Currents

AGU/fm2020/SHO29.20
part.2

C. Fred Driscoll
UCSD Physics

0) $B_{\mathrm{RMS}} \propto \Gamma_{\mathrm{w}}{}^{0.75}$ over $1 \to 5\mathrm{AU}$

Local Electric Currents are the dominant source of B(t) at spacecraft

1) Pervasive Random Fluctuations

--- Spectrum is random as f^{-1} above 10^4 μHz ($\tau < 100.\mathrm{sec}$)

--- "DC" values ($f < 10.\mu\mathrm{Hz}$, $\tau > 1.\mathrm{day}$) scale as "Mean of random walks"

2) $B_r(t)$ and $B_\theta(t)$ are sometimes *Correlated,* by distinct Fourier components at f_{Rot}

--- Highly variable : 1% - 30% (avg 12%) of B^2 Energy; not a persistent Spiral .

--- Removing *single* f_{Rot} component eliminates (r-θ) Correlation

---?? From gradient of North-South Current, driven by N-S charge imbalance

3) "Dynamical Arcs" are prevalent in the data :

--- Causes Non-random Spectral Energy $10^1 < f < 10^3$ μHz

--- Well-modelled by "Double Filament" radial Currents

--- Similar to PSP "Switchbacks" seen at 0.1 AU

Measurements :
-- ACE @ .99AU
-- Ulysses @ 1 – 5 AU
-- Mariner @ 0.3 – 1 AU

p^+, e^- : $v_w \sim 500.\mathrm{km/s}$

$n_w \sim 10^{6.8}\ \rho^{-2}\,[\#\#/\mathrm{m}^3]$

Flux $\Gamma_w \sim 10^{12.5}\ \rho^{-2}\,[\#\#/\mathrm{s}\cdot\mathrm{m}^2]$

$\rho \equiv r\,/\,1.\mathrm{AU}$

$\mathcal{E}_{p+} \sim 1.3\,keV$

$\mathcal{E}_{e-} \sim 10.eV$

Supported by UCSD and AFOSR

(0) Magnetic Fluctuations Levels are Determined by the Local Solar Wind Flux Γ_w

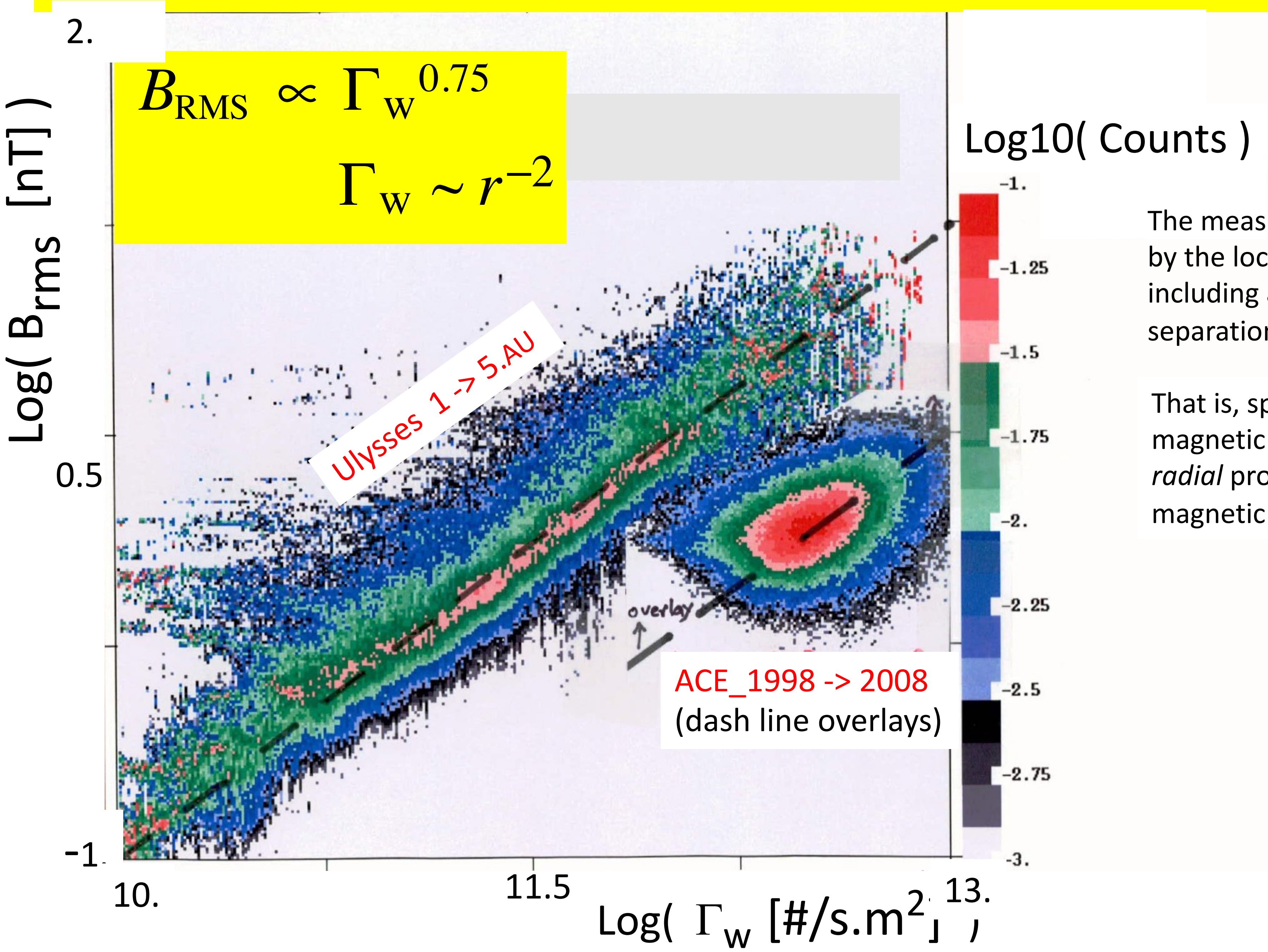

The measured magnetic fluctuations are created by the local electrical-currents of the Solar Wind, including any global currents from global charge separation.

That is, spacecraft observations of notable magnetic fluctuations appear after the SW particle *radial* propagation time, unrelated to "rooted spiral magnetic field" lengths or geometries.

Spectrum of Magnetic Fluctuations : ACE MAG @ 1.AU

16.sec data, 1998.0 -> 2019.4

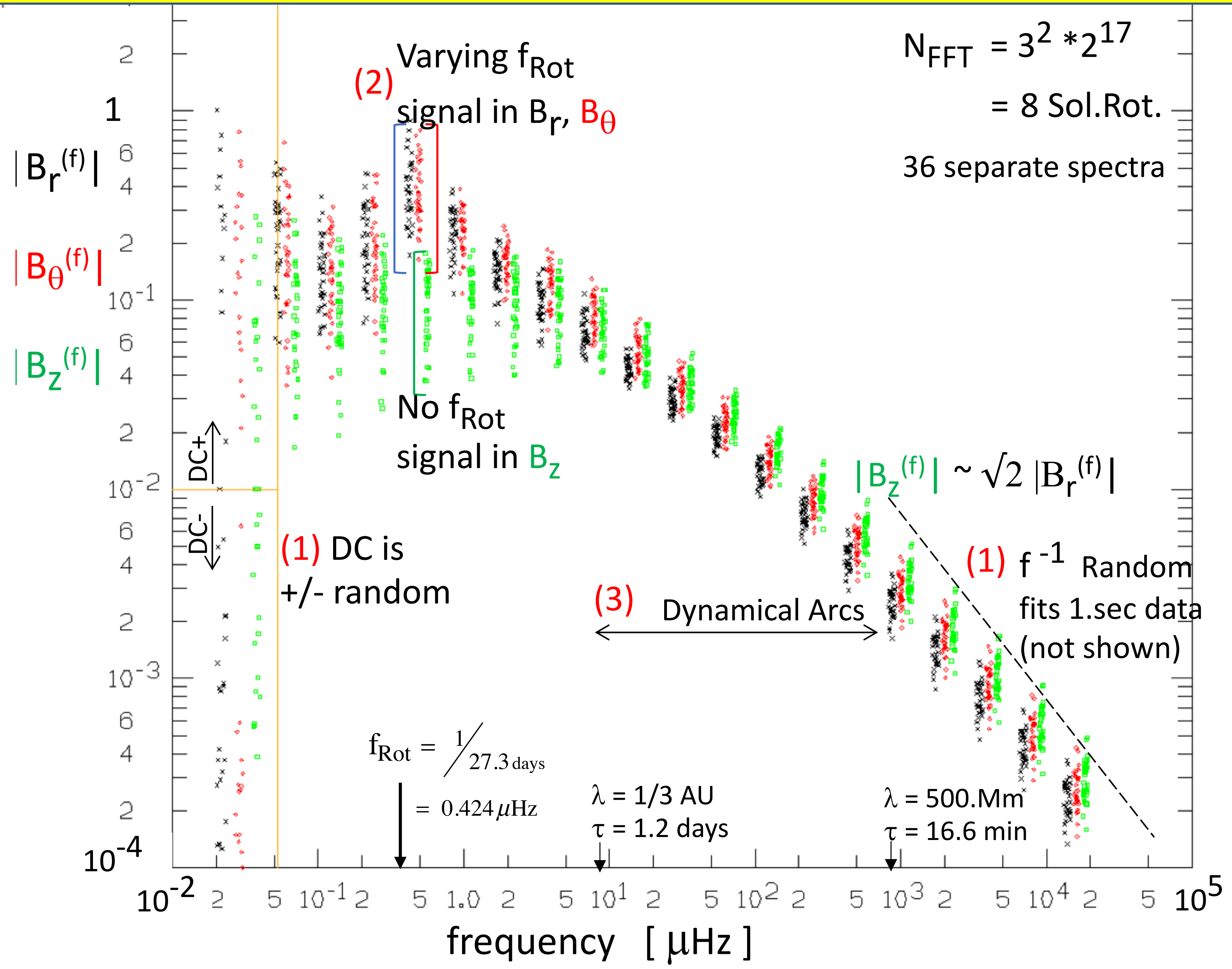

(1) Low-frequency and High-frequency components show "random walk" spectra

(2) $f^{\,Rot}$ components are *exceptional* : highly variable, providing sole $B_r - B_\theta$ correlation

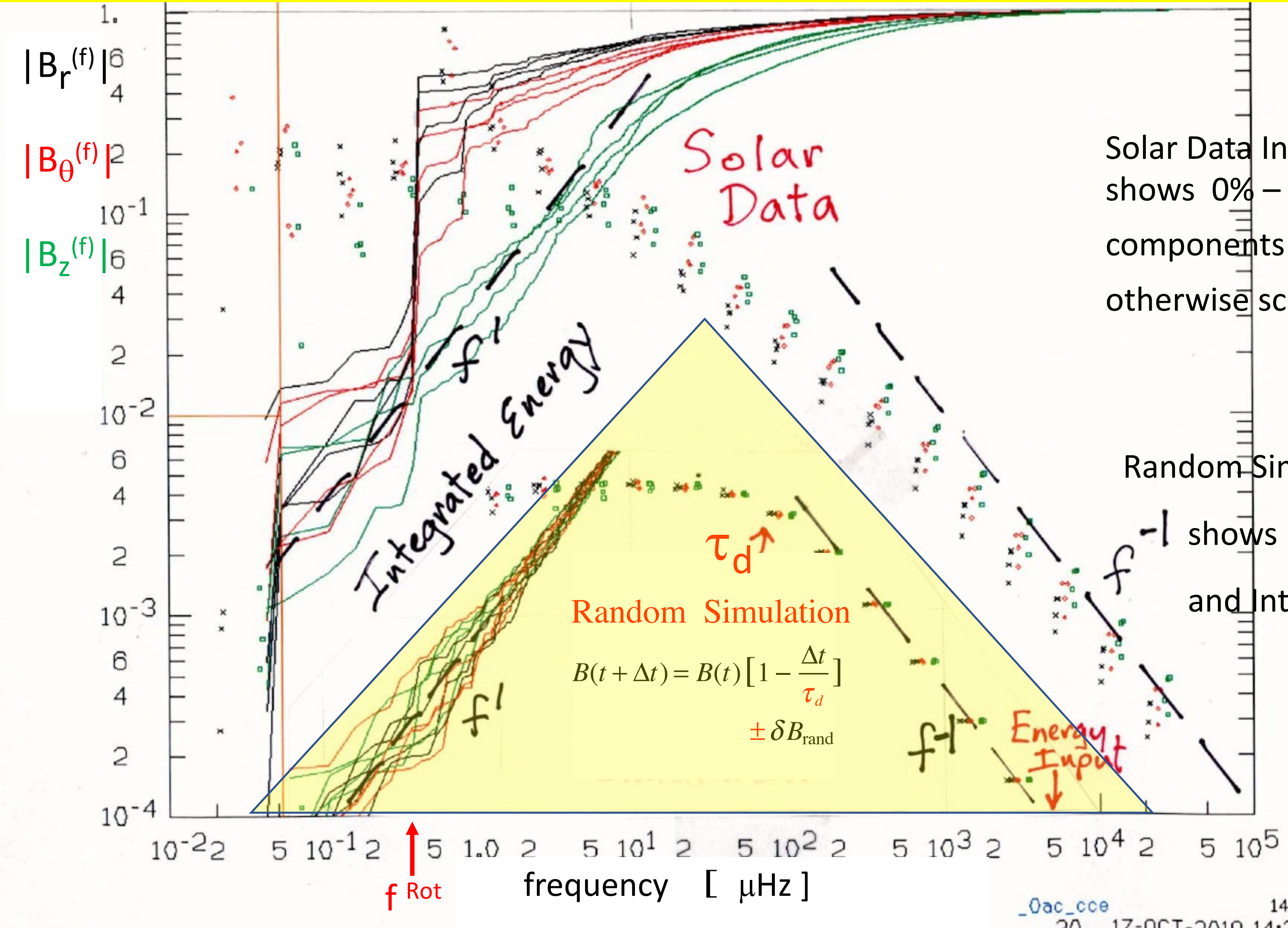

4 spectra

Solar Data Integrated Energy shows 0% – 30% spike in components at f^{Rot} ;and otherwise scales up as $f^{\,1}$.

Random Simulation with Dissipation at τ_d shows $f^{\,-1}$ and $f^{\,0}$ spectral regions; and Integrated Energy scales as $f^{\,1}$.

(1) There are no significant "persistent" magnetic fields at 1.AU :
"DC" levels vary +/- as expected from random higher-frequency "drives"

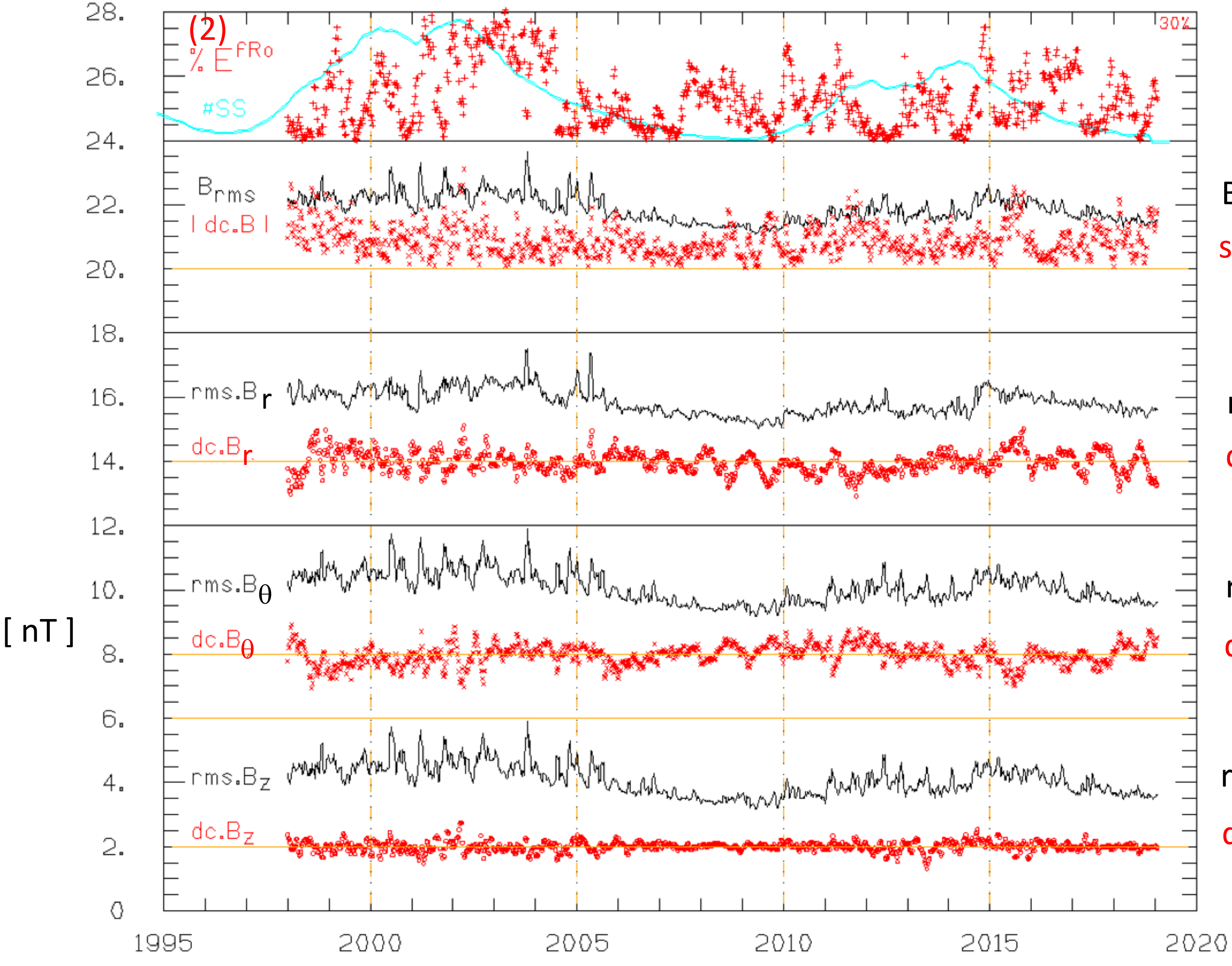

Tavg = 1.Sol.Rot

B_{rms}

$\mathrm{sqrt}(dcB_r^2 + dcB_\theta^2 + dcB_z^2)$

rms. B_r

dc. B_r

rms. B_θ

dc. B_θ

rms. B_z

dc. B_z

(2) Spectrum of Magnetic Fluctuations : ACE MAG @ 1.AU

16.sec data, 1998.0 -> 2019.4

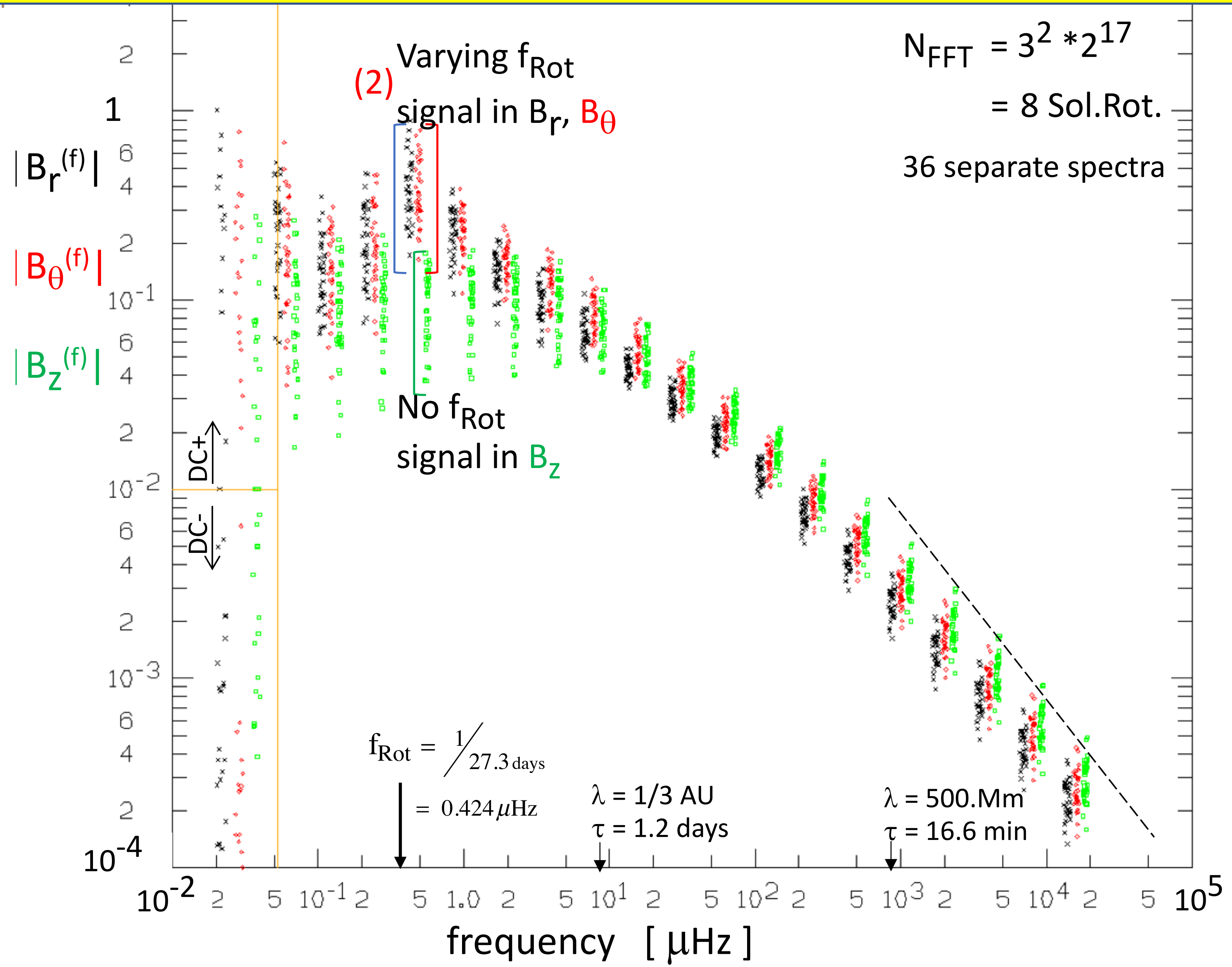

Spectra of ACE/MAG Br and Bθ display temporally variable (but correlated) distinct components at fRot, with weaker but occasionally distinct components at harmonics of fRot . No similar components are visible in Bz .

(2) Fluctuating B_r^{fRot} and B_θ^{fRot} are *phase-Correlated* ; B_z^{fRot} is noise.

0% –> 30% of Magnetic Energy is in B_r^{fRot} and B_θ^{fRot} fluctuations.

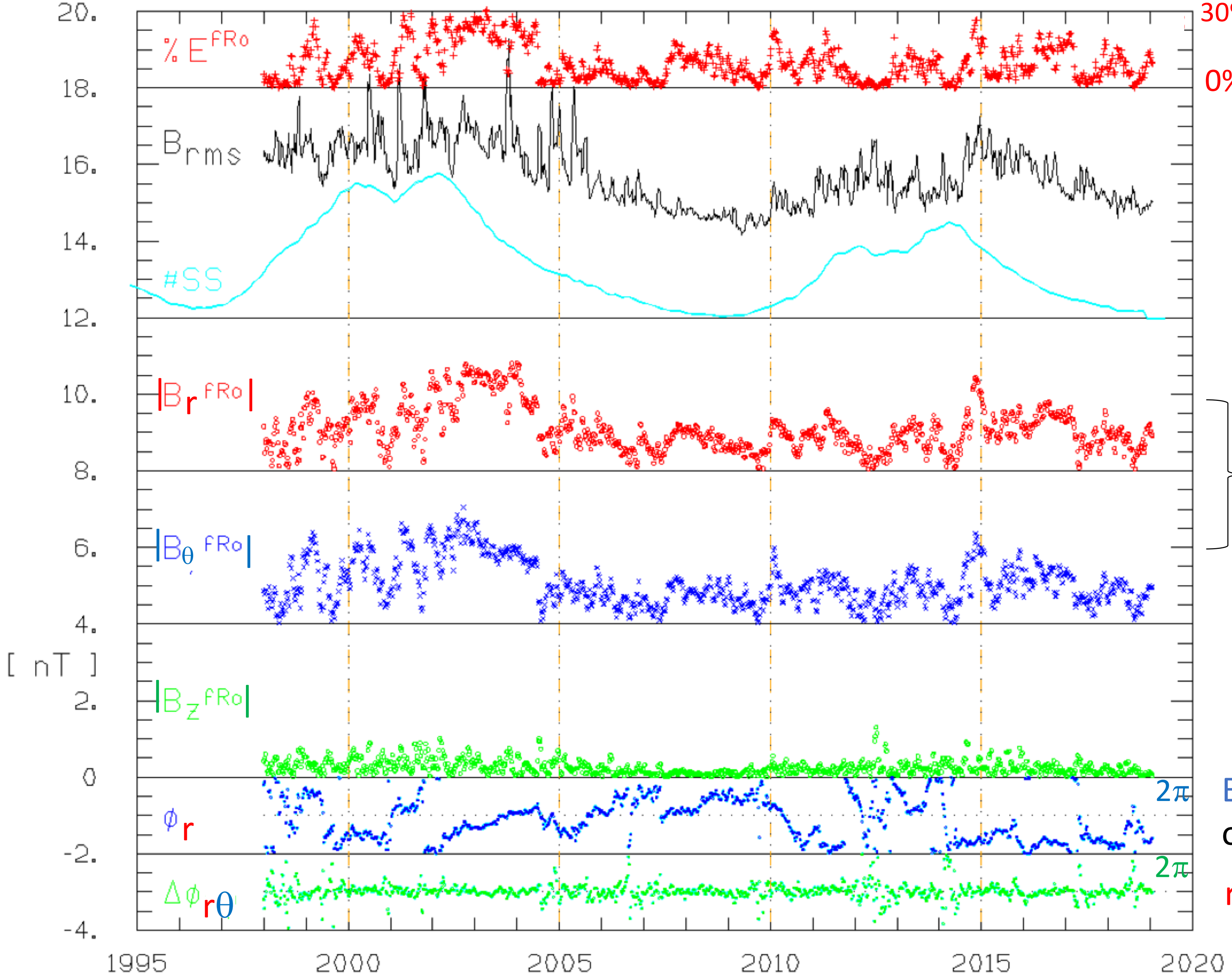

30% Energy in f^{Rot}

0% components

$|B_r^{fRot}|$ and $|B_\theta^{fRot}|$ both vary on 3-month time scale

B_r Phase may be "steady" over several solar rotations

$r\theta$:180° phase difference

(2) Radial Dependence of fluctuating components B_r^{fRot} B_θ^{fRot} B_z^{fRot}

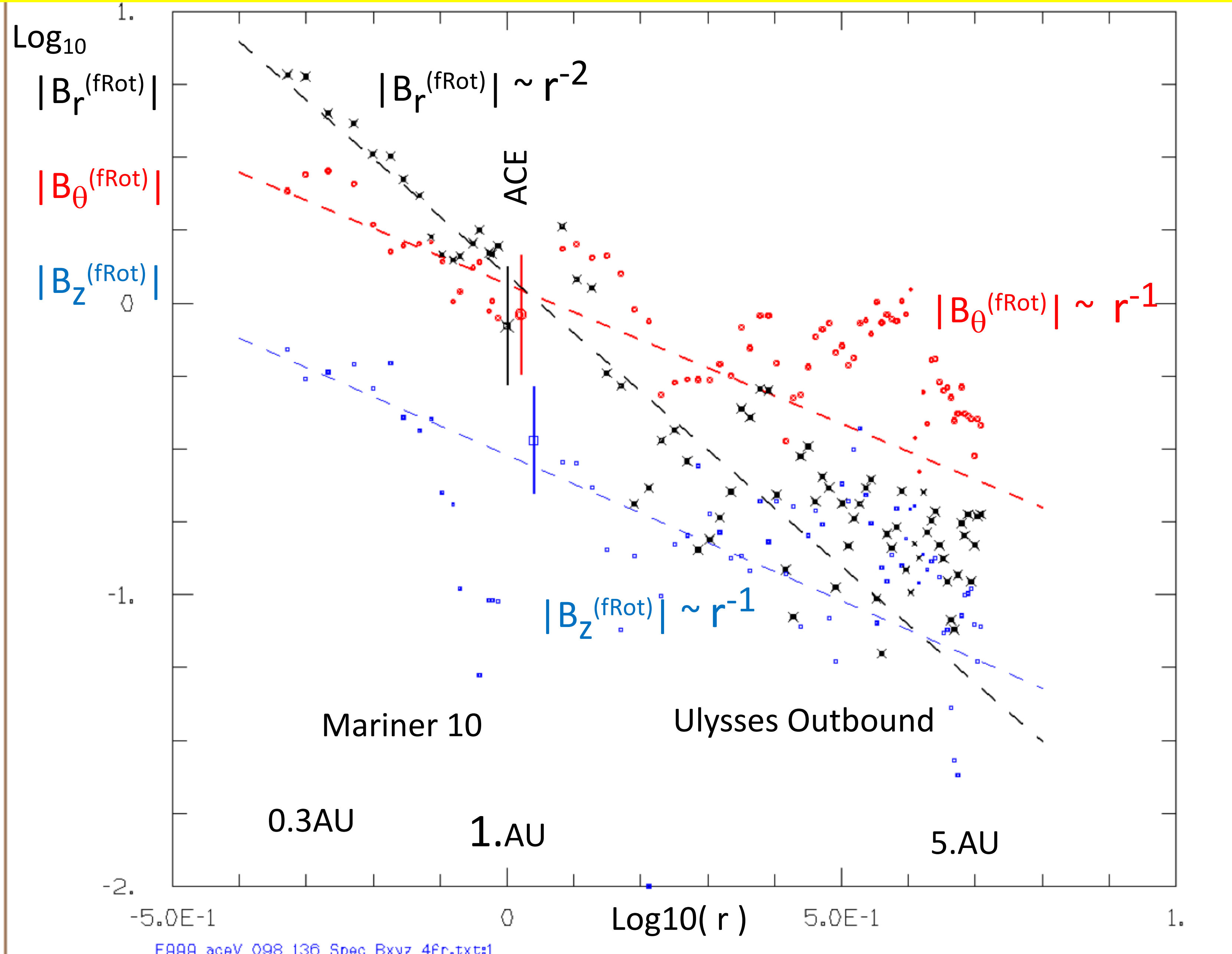

Sparse data from Ulysses outbound and Mariner 10 allows estimates of the radial dependence of the fRot components, albeit polluted by the (unknown, quasi-random) temporal variations.

The 20-year ACE averages and standard deviation levels are shown at 1.AU

Solar wind dynamic and fluctuation characteristics probably determine $|B_r^{(fRot)}| \sim r^{-2}$, $|B_\theta^{(fRot)}| \sim r^{-1}$, and $|B_z^{(fRot)}| \sim r^{-1}$.

(2) $B_r - B_\theta$ anti-Correlation is *Removed* when the Fourier Components at f_{Rot} are *Removed*

Histograms of { $B_r(t)$, $B_\theta(t)$ } pairs

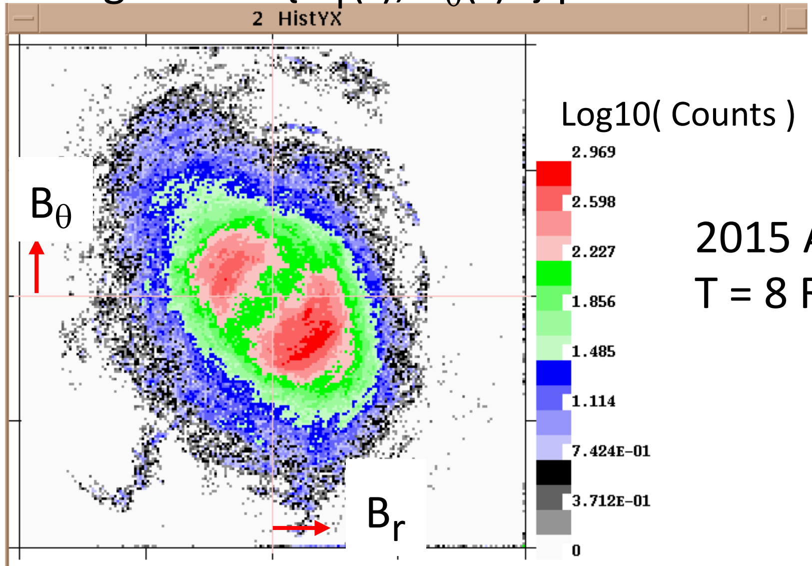

2015 ACE Data,
T = 8 Rotations

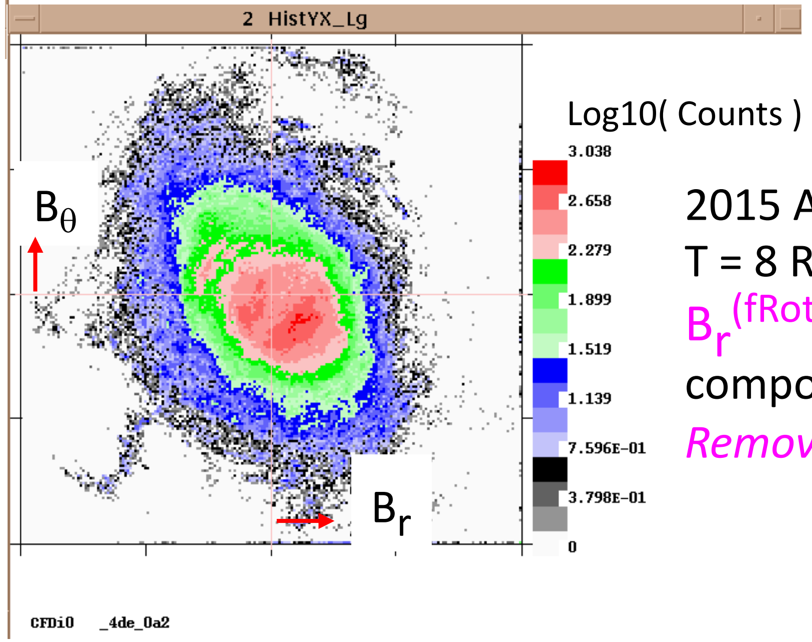

2015 ACE Data,
T = 8 Rotations, with $B_r^{(fRot)}$ and $B_\theta^{(fRot)}$ components artificially *Removed* from the data

Only in the f_{Rot} components is there a variable-strength B_r-B_θ anti-correlation, which has been mis-interpreted as a persistent magnetic spiral. This isolated correlation is seen for any chosen integer period T .

These components represent temporal variations in the local particles, currents and fields as global + / − solar surface source variations rotate past the (essentially stationary) satellite.

Granulation :
L ~ 1. Mm
Macro-Granulation
L ~ 20.Mm ?

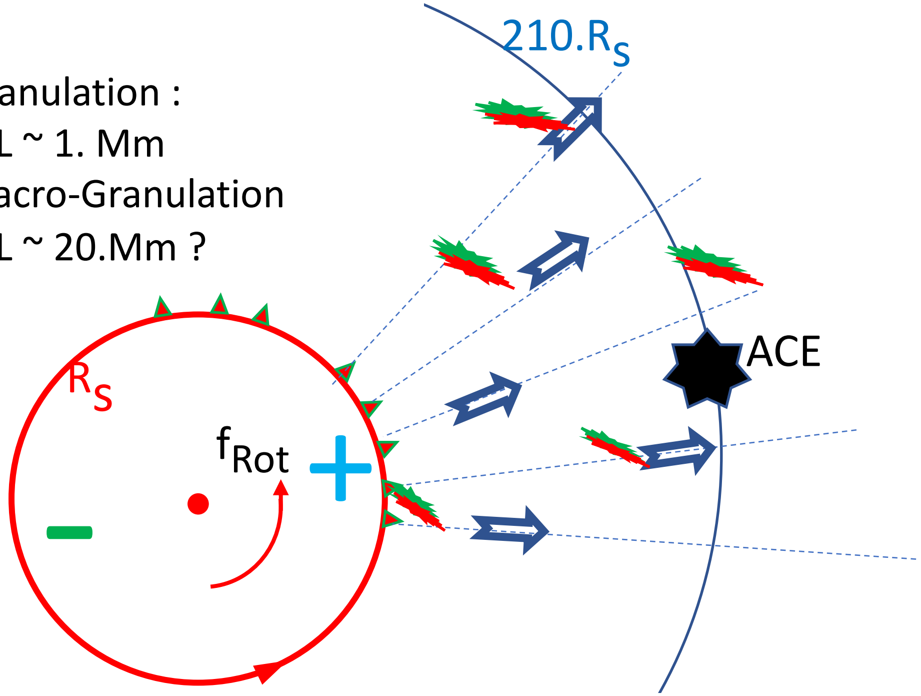

(3) "Dynamical Arcs", Constant Magnitude temporal "arcs" in (B_θ, B_z), (B_θ, B_r), or (B_r, B_z)

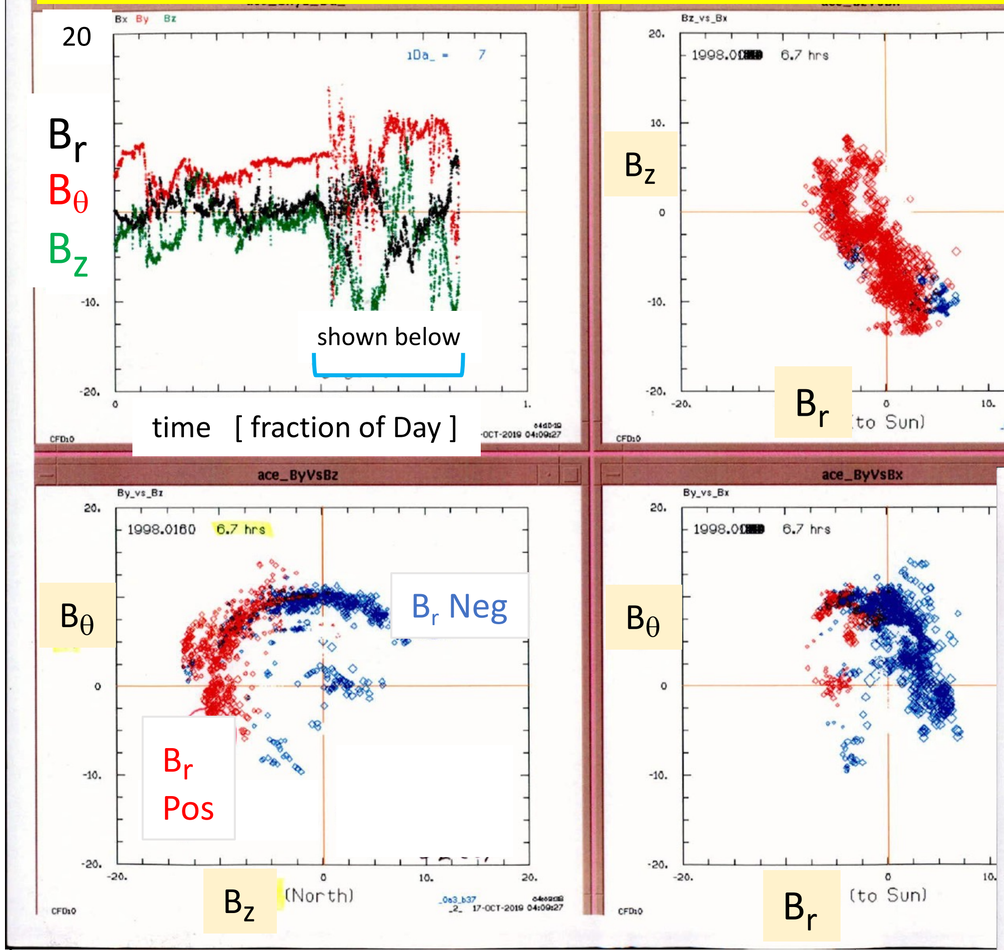

At left, a {Bθ,Bz} constant magnitude Arc appears in 6.7 hours MAG temporal data, unrelated to the sign of Br (red/blue). Other pairs {Bz,Br} and {Bθ,Br} show no Arc during this time, but are equaly prevalent in general. Below are 4 Arcs of 1.3 hrs duration, selected for their "clean" appearance.

Below left is a 0.2 hr segment from PSP data showing similar behavior, albeit at 20x larger field magnitudes.

ACE 4 Examples

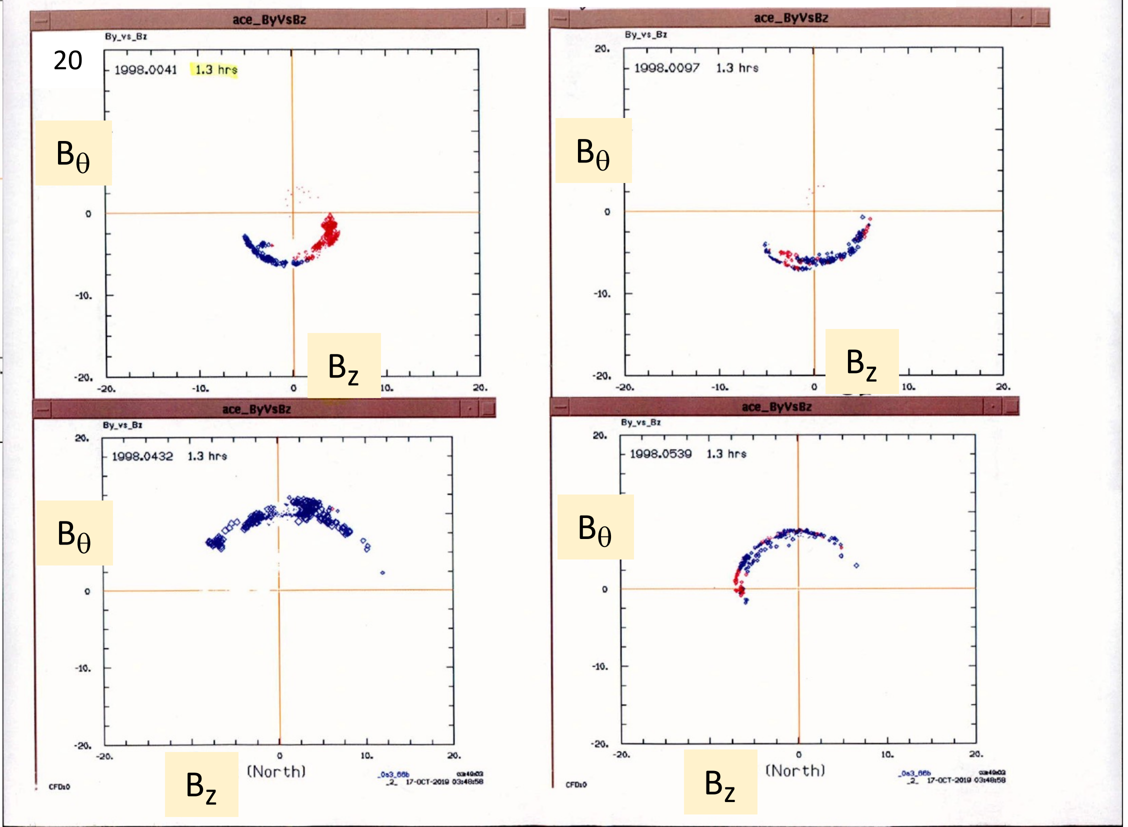

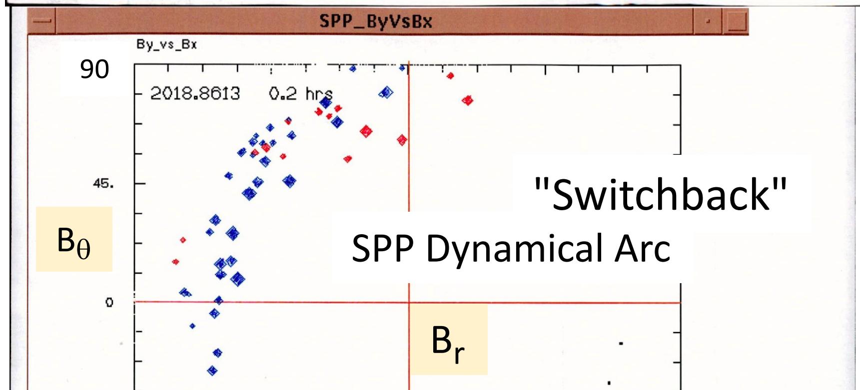

(3) ACE MAG : 137,000 "Dynamical Arcs" in 21 years. T ~ 0.5 hr
All orientations : Bθ–Bz , Br-Bz, Br-Bθ . Rate ~ 18/day

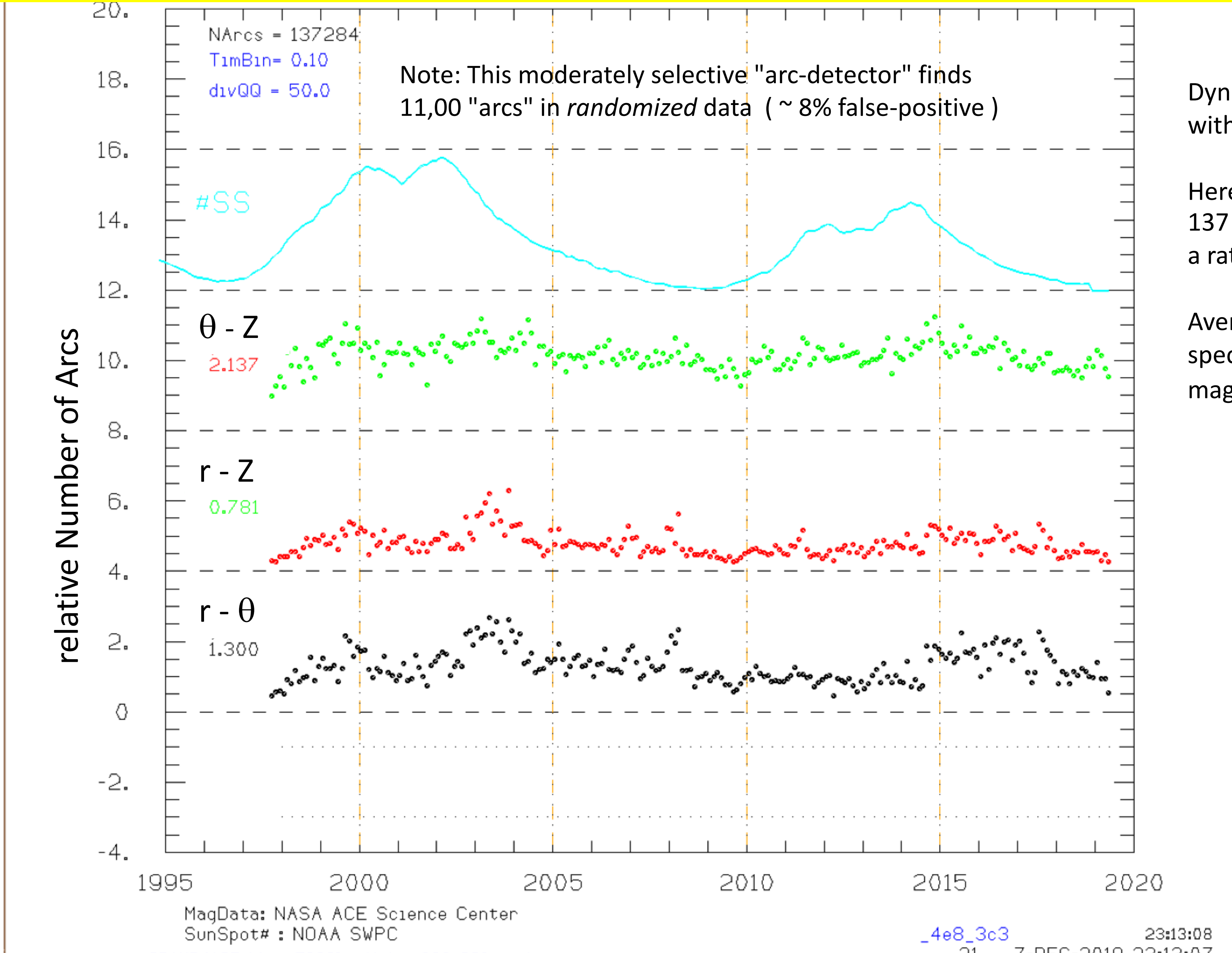

Dynamical Arcs appear in all pairs of {Br, Bθ, Bz}, with similar rates of occurence.

Here a moderately selective computer filter counts 137 000 Arcs (+/- 10%) with periods T~0.5hr, giving a rate of 18/day.

Averaging over multiple Dynamical Arcs contributes to the spectral region of $10 < f < 1000\ \mu$Hz, where field magnitudes fall off more slowly than the "random" f^{-1} .

(3) Dynamical Arc Model : Double Electrical Current Filaments

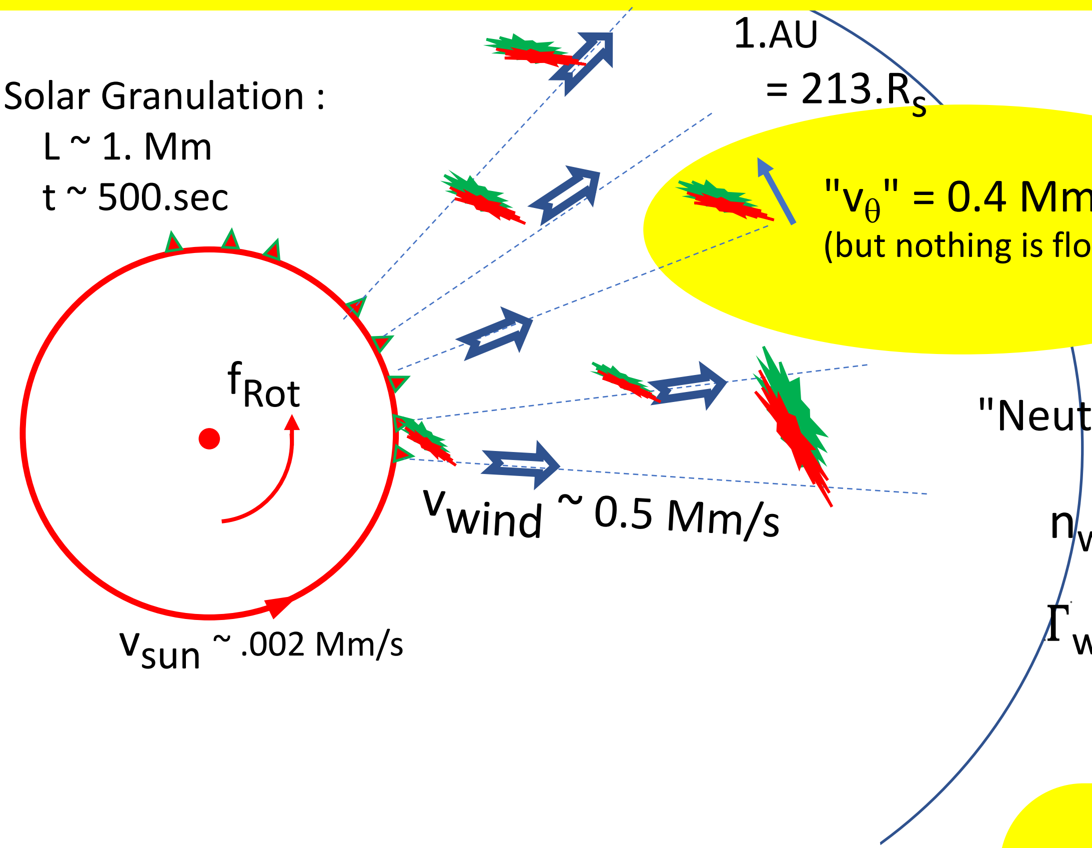

"Neutral" Flow" of { p+, e- }

$n_w \sim 10^{6.8}$ [##/m^3]

$\Gamma_w \sim 10^{12.5}$ [## /s.m^2]

$\sim 10^{24.5}$ [##/s.(Mm)^2]

Spacecraft measurements establish that the Solar Wind e-/p+ particle flux is basically radial , and global charge conservations requires that it is basically charge-neutral.

However, small deviations from charge neutrality ($\alpha \sim 10^{-5}$ here) can create currents which create the 5.nT magnetic field magnitudes observed at 1.AU.

Here, the spatial scale of $r_0 \sim 10^3$ Mm is suggested by the 0.5 hr time scale for major B-field magnitude changes.

The "challenge" is to characterize propagating structures of low-collisionality neutral currents and electric currents, with self-consistent and Electric and Magnetic fields.

Suppose $\delta n = (n_+ - n_-)$

$== \alpha \; n_w$

from Filamentation, Dynamics, Current Pinch

Then

$$B \approx \frac{2}{c\,r} (\alpha \, e \, n_w \, v_w) (\pi \, r_0^2)$$

B ~ 5. nT implies :

α	r_0	$\tau = v_w r_0$
10^{-3}	10^{1}Mm	20.sec
10^{-5}	10^{3} Mm	0.5 hour

dominant in data

(3) Two Filament Simulation (+ / - Currents) propagating radially gives "Dynamical Arc" signature

v_r = 0.5Mm/s

time = 500.sec

length = 200.Mm

Tilt = 30°

+ / - Separation

~ 5.Mm

Currents "fuzzy"

by ~ 10.Mm

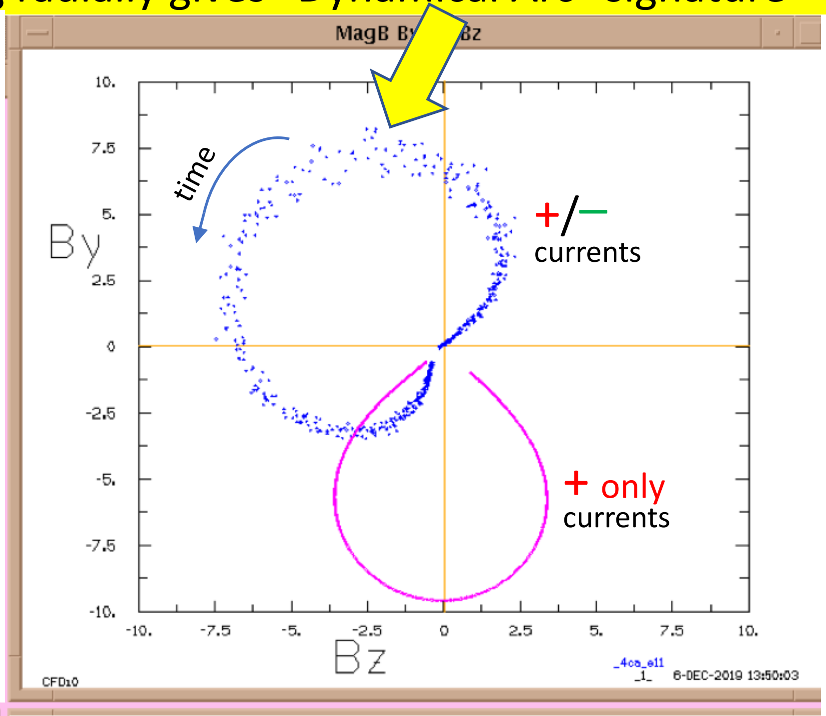

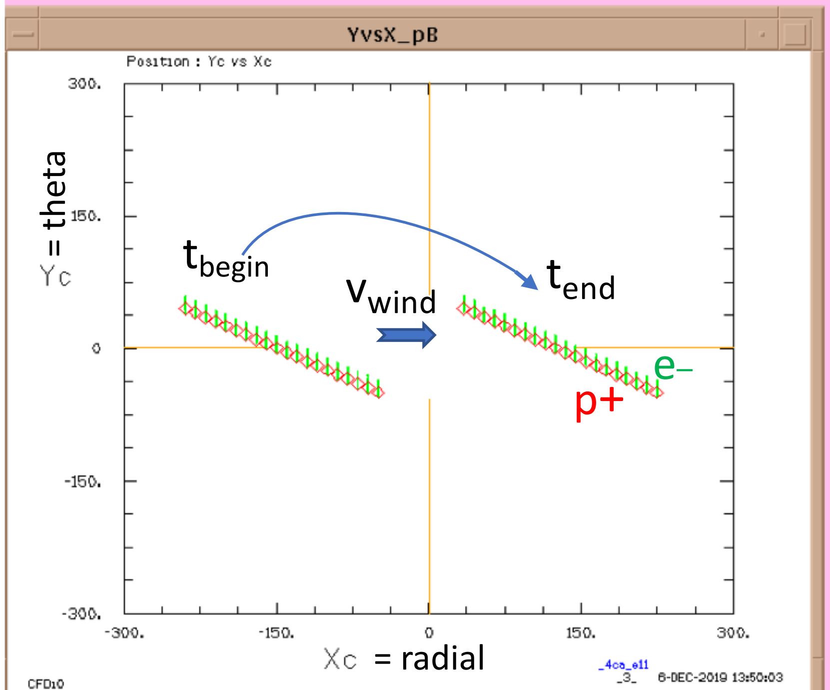

A simple "geometric" calculation of magnetic fields shows that Dynamical Arcs in pairs of {Br, Bθ, Bz} will arise from radially propagating charge separations.

Here, 200.Mm long filaments of +/- charge, separated by 5.Mm, propagate radially past the spacecraft with v_r = 0.5Mm/s .
The currents are modelled by hundreds of particles, each "fuzzy" over 10.Mm.

The broad Dynamical Arc signature is obtained when the total charge is Zero; but not when only one sign of current is included.